International Research Journal of Engineering and Technology (IRJET) e-ISSN: 2395-0056
Volume: 09 Issue: 09 | Sep 2022 www.irjet.net p-ISSN: 2395-0072

Investigation of PolyMethyl Methacrylate for Speedometer Application

Sajal Anand[1], S.S Ohol[2], Subhajit Basu[3]

[1]*Student, College Of Engineering Pune, Maharashtra*
[2]*Associate Professor, Department Of Mechanical Engineering, College Of Engineering Pune, Maharashtra*
[3]*Lead COC, Varroc Engineering* Limited, Pune, Maharashtra

Abstract - *This paper presents investigation of PMMA grade material for use in a Two-wheeler speedometer lens application. Of all the various components that make up the speedometer the lens is directly visible to the rider and hence correct and clear display of information is important as it directly affects their decision making. Mold flow analysis is carried out to establish the molding parameters and defects if any. From the risk assessment derived from the DFMEA and customer specific test standards CAE analysis has been carried at loading conditions of tightening torque of two different cases, modal analysis and harmonic response are simulated to check for any adverse stresses and deformations for any fouling and cracking at lens within frequency range of interest.*

Key Words: **Polymethyl Methacrylate, Speedometer, Mold Flow, CAE, Modal Analysis.**

1. INTRODUCTION

A speedometer or speed meter is a gauge meter that measures and displays the instantaneous speed of the vehicles. A traditional speedometer is of mechanical type also called as eddy-current type; a flexible cable driven by the gear linked at transmission. When the vehicle is in motion, a gear assembly turns the speedometer cable. A small permanent magnet affixed to the cable interacts with a small aluminum cup (called a speed cup) attached to the shaft of the pointer on the analog speedometer instrument. As the magnet rotates near the cup, the changing magnetic field produces eddy current in the cup, which themselves produce another magnetic field. With the advancements in the field of mechatronics and development of sensor technology traditional mechanical speedometers were replaced by digital speedometers. Small magnet attached to the car's rotating drive shaft sweep past tiny magnetic sensors (either reed switches or Hall-effect Sensors) positioned nearby. Each time the magnets pass the sensors, they generate a brief pulse of electric current. An electronic circuit counts how quickly the pulses arrive and converts this into a speed, displayed electronically on an LCD Display. A speedometer under study is an assembly of the following components transparent cover lens, CR sponge Sealing ring, Printed dial, Reflector with tell tale symbols, PCB with electronics and stepped motor, housing/casing and wiring harness.

1.1 LENS AND MATERIAL

The Lens forms the transparent cover at the visible side of the cluster and its primary function is to provide clear and transparent display of the data to the rider under all environment circumstances while taking in the vehicle operational vibration and loads.

The concerned lens has 4 vehicle mounting locations with ribs designed to control warpage during manufacturing and also serve as load bearing geometries with its design thickness and height as per guidelines mentioned in the standards mentioned before. The Lens-Housing subassembly is achieved through self-tapping screws at 5 locations along with locators. The concerned lens also has the trip button interference fitted onto the class A surface with class B surface having a coating of Antifog

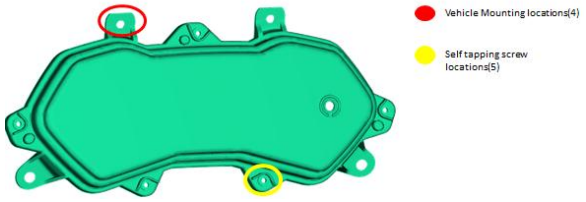

Figure 1: Lens with 4 vehicle mounting locations and 5 self-taping screw sub assembly mountings

By nature of the application the PMMA will be subjected to various requirements in the form of its transparency, degradation retarding properties mainly UV resistance and water absorption, and since the component will be subjected to various loads and vibration mechanical properties will play a crucial role.

Based on the general material requirements of a lens, various amorphous polymers were studied for their properties and PMMA was chosen as material of choice.

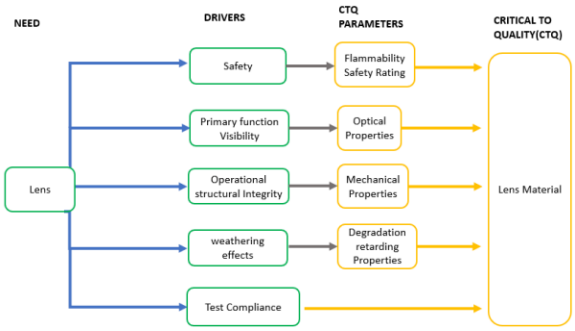

Figure 2: Parameters for material selection

2. MOLD FLOW ANALYSIS OF LENS WITH PMMA

The objective of the analysis is to carry out FILL+PACK+WARP analysis for the component using an industry grade PMMA. Initial molding parameters will be established and any aesthetic defects can be addressed. AUTODESK Mold flow 2021 has been used for this analysis. Dual Domain mesh has been carried out followed by adding 10 layers of 3D tetras. The aspect ratio is to be maintained within 100, the total 779642 tetrahedral have been generated. The recommended molding conditions from the software are as follows,

Mold surface temperature	75	C
Melt temperature	235	C
Mold temperature range (recommended)		
Minimum	60	C
Maximum	90	C
Melt temperature range (recommended)		
Minimum	220	C
Maximum	260	C
Absolute maximum melt temperature	270	C
Ejection temperature	94	C

Figure 3: Recommended processing conditions

A cold sprue edge gate has been used with width and thickness as 16mm and 1.4mm respectively. Packing profile has been set as 80% of the injection pressure for 10 seconds.

It takes 2.66 seconds to fill the cavity with no observed short shots. Areas colored red are the ones filled towards the end are subject to more shrinkage due to lack of packing.

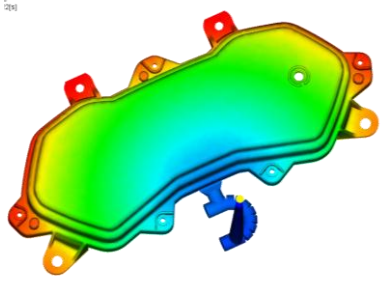

Figure.4 Fill time plot

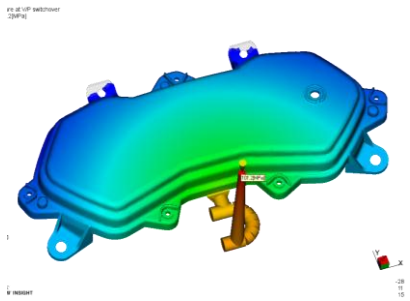

Figure 5: Injection Pressure

The maximum pressure observed during the filling phase is 101.2 MPa which well below the machine limit of 120 MPa.

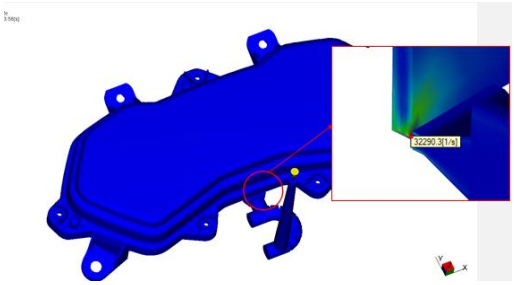

Figure 6: Shear Rate

The shear rate is a measure of the rate of slip between different layer so polymer material, shear rate generates temperature which is desirable for viscous material like PMMA to enable better flow however too large shear rates can cause material degradation. The shear rate observed is 32290.3(1/s) which is below 4000(1/s).

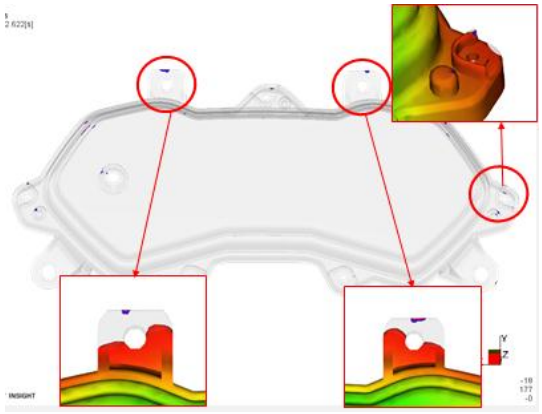

Figure 7: Air traps

Air traps (end fill locations) and unavoidable weld lines are observed at areas furthest from the gate as expected as these regions are filled last and flow fronts meet. Air traps can be avoided by providing venting at these points, although the weld lines are unavoidable they are at temperatures above the melt temperature as shown

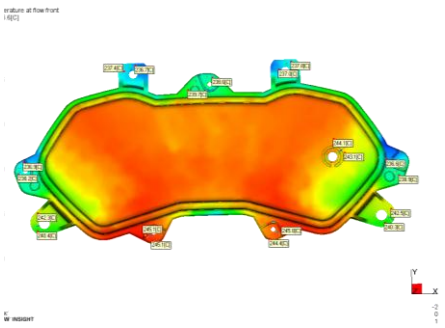

Figure 7: Temperature plot

The shear along the mold walls and the shear rate cause temperatures to rise within the melt decreasing its viscosity, the melt temperature was set at 235°C and maximum temperatures observed are 10°C above, no drop of temperature is observed hence weld lines are strong.

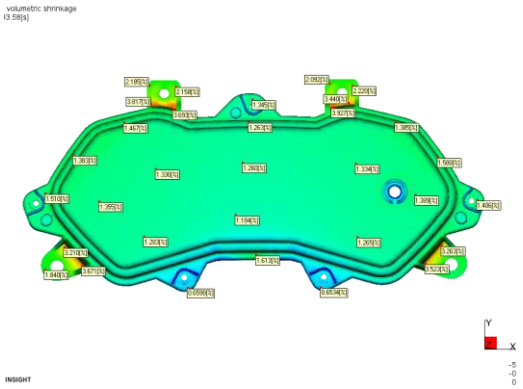

Figure 8: Volumetric shrinkage

The volumetric shrinkage plot shows variable shrinkages which are due to variable thickness geometry. The thicker sections undergo more shrinkage as the cooling time within the mold is not sufficient, moreover the portions of geometry further away from the gate witness more shrinkages due to the lack of packing. Multiple gates and more packing time/pressure can be provided to reduce the values.

Deflection plots due to differential shrinkage alone are plotted in X,Y & Z directions individually as shown.

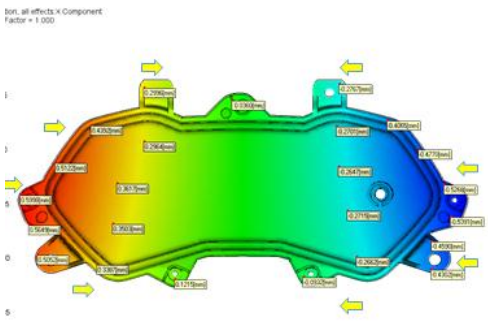

Figure 9: X direction deflection

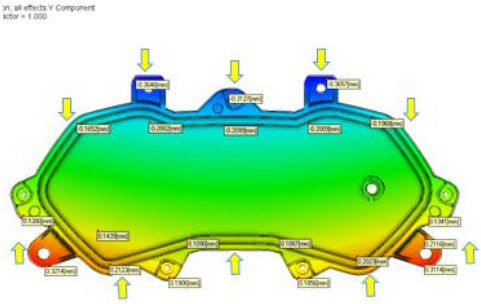

Figure 10: Y direction deflection

Figure 11: Z direction deflection

The deflections in X(figure 9) direction are +0.6mm and -0.59mm which are symmetric as desirable, moreover maximum deflections are observed in areas further from gate due to lack of packing. However these deflections are within the limits of allowable shrinkages derived from DFMEA. The maximum deflections in Y direction (figure 10) are +0.35mm and -0.38mm which are both symmetric and within limits. Deflections in Z direction (figure 11) are more in thicker regions which are explained as lack in proper cooling time, also the flappy parts are therefore designed with ribs to minimize warpage in Z direction, maximum values of deflections observed are +0.23mm and -0.14mm which are within limit.

3. STRUCTURAL ANALYSIS OF COMPONENT WITH PMMA

Materials usually exhibit a fixed melting temperatures for polymers the temperature at which hard glassy state of an amorphous material changes to rubbery state is called as the glass transition temperature Tg. As the temperature of the material reached Tg its behavior changes from viscoelastic to viscoplastic. The Tg value of our chosen PMMA grade is 117°C but since our component is exposed to temperatures much below the Tg material non linearity is unaccounted for and linear static analysis is carried out. Moreover, since the rise in temperature induces softness and hence a drop in yield stress a FOS of 2 is a reasonable parameter to account for in our analysis.

Loading and boundary conditions are as follows,

From the customer specifications and DFMEA done the tightening torque values at the Speedometer assembly-vehicle mounting locations have been taken as 1**.3 Nm**. The poission's ratio of 0.35, yield stress and Young's modulus have been derived from the material data sheet. **BETA CAR ANSA** has been used for Pre-processing and meshing with a global edge length of 2mm, **MSC FEA 2020** has been used as solver and post processor.

To calculate the equivalent clamping force as a consequence of the tightening torque is calculated as

$$T = K \times F \times d \times (1 - I \div 100)$$

Where,

T= Tightening torque

K= Constant based on bolt material

d= Nominal diameter of the bolt

I= Lubrication factor.

On entering the relevant values we get **F= 1300 N**.

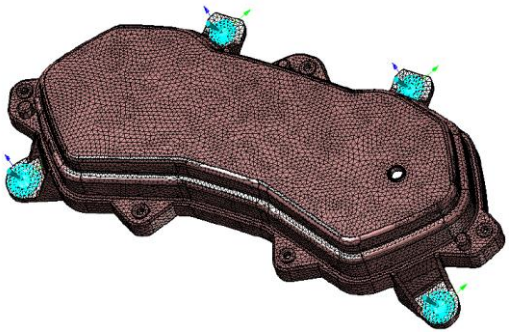

Figure 12: Loading at 4 vehicle mounting location

The figure 12 shows the 4 mounting locations at which the 1300N equivalent clamping force has been applied using NASTRAN based RBE 2 Stiffening elements with salve nodes taken at washer. The boundary conditions are used to arrest the 6 Degrees of freedom on the class B surface of the lens as shown in figure 13.

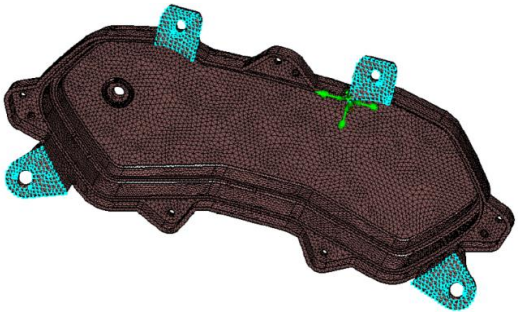

Figure 13: Arresting Degree of Freedom

The Von mises stress induced as a consequence of tightening are shown in the figure 14.

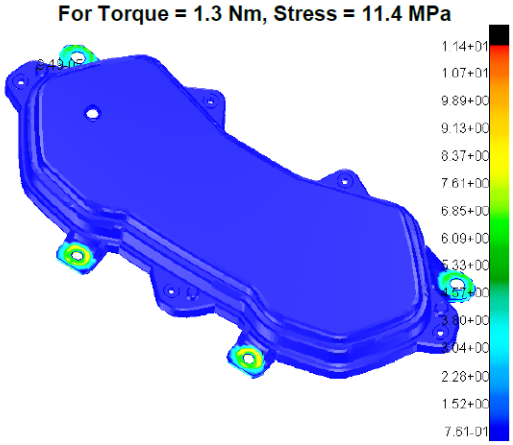

Figure 14: Von Mises Stress

The maximum stress values observed are 11.4 MPa which are below the permissible limit by 70% calculated using a factor of safety of 2.

At the 5 self-tapping screw locations a similar static structural analysis is carried with the same meshing conditions, the equivalent clamping force however is calculated using,

$$T = F[\frac{p}{2\pi} + \frac{\mu 1}{\cos \beta} \times \frac{(Ds + Dh)}{4} + \mu 2 \times \frac{(Dn + Dsh)}{4}]$$

Where,

p- Pitch

μ1- Friction coefficient at screw-lens surface

μ2- Friction coefficient at screw-casing surface

Ds- nominal diameter of screw

Dh- Diameter of casing surface

Dn- Diameter of lens surface

Dsh- Diameter of screw head bottom.

Putting in the values for a tightening torque value of 0.45 Nm and friction coefficient of 0.7 the equivalent clamping force **F= 250N**

The loading conditions using the RBE 2 elements are shown in figure 15 while the arrested degree of freedom class B surface is shown in figure 16.

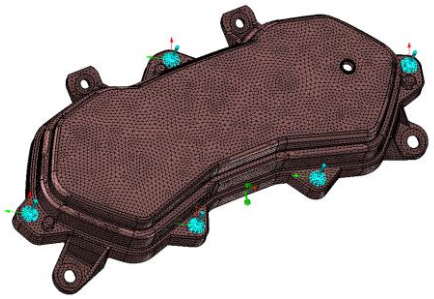

Figure 15: Self tapping screw loading

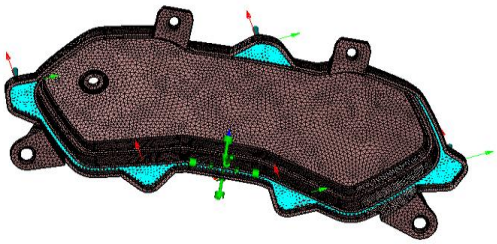

Figure 16: Self tapping screw boundary conditons

The Von mises stress generated as a consequence of this tightening torque is shown in figure 17,

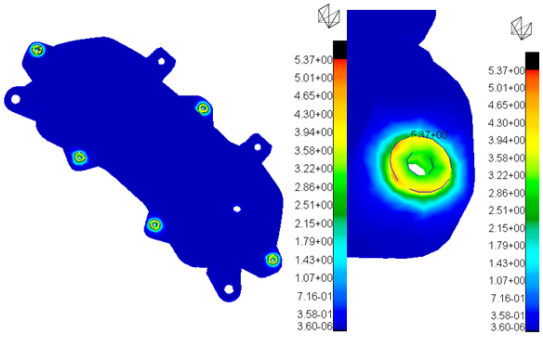

Figure 16: Von Mises Stress Values

The maxim Von mises stress value is 5.37 MPa which is well below the permissible limit by 86%

4. MODAL ANALYSIS OF SPEEDOMETER WITH EQUIVALENT MASS

For the modal analysis materials are assigned to the different components of the speedometer assembly in the CATIA V5 software. An equivalent mass of 173 grams of the internal subassemblies is placed on the center of gravity. Using the BETA CAE ANSA meshing is carried out for the Lens and the housing with NASTRAN based RBE 3 elements connecting the equivalent masses to the housing mounting locations as shown,

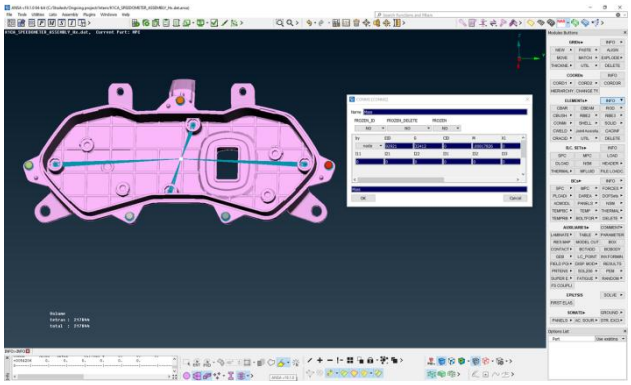

Figure 17: RBE 3 elements to connect equivalent mass

The 4 vehicle-speedometer assembly mounting locations are connected using RBE 2 elements. Carrying out the free-free modal analysis all the 6 degrees of freedom are arrested at the point to avoid the first 3 rigid body motion accounting as modal frequencies to be 0. The free –free modal analysis was carried out using BETA CAE EPILYSIS as solver and BETA CAE META as post processor. The resulting modal frequencies are observed and frequencies within 50-500 Hz are of further investigation based on the test standards employed by the customer. The table below gives the modal frequency output,

Mode	Frequency(Hz)
1	382.03
2	517.46
3	710.50
4	767.20
5	785.77
6	857.45
7	922.67
8	1070.51
9	1132.33
10	1223.40

Table 1: Modal Frequencies

Modal frequency of interest within the range of 50-500Hz is 382.03Hz.

5. HARMONIC RESPONSE

The harmonic response of the speedometer is lens-housing and equivalent mass subassembly is carried out with 10g of acceleration in X,Y,Z directions individually at frequency ranges of 50-500Hz and first modal frequency using damping ratio of 5%.

The allowable deformations in the X&Y direction are 0.5mm while in the Z direction is 5mm as mentioned in the DFMEA. Moreover, the stress induced is compared against the fatigue limit value of σy /4 for our chosen PMMA grade. The software displays the frequency at which the deformation is maximum. For the X direction the response of the system is maximum at 382.03 Hz and the stresses generated are shown below,

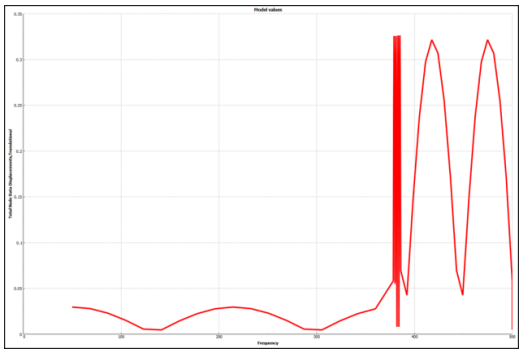

Figure 17: Displacements in X direction

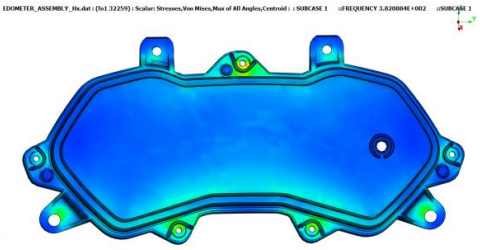

Figure 18: Stresses on Lens in X direction

The maximum value of displacement observed in X direction is 0.32 mm which is below the limit of 0.5mm while the stresses generated as shown in figure 18 are 5.65 MPa which is below the material fatigue limit by 70.57 %.

The Maximum displacements occurring in Y direction take place at frequency of 500Hz while the maximum stresses generated on the lens amount to 0.61 MPa only both of which are under the permissible limit. They have been shown in figures 19 and 20 respectively.

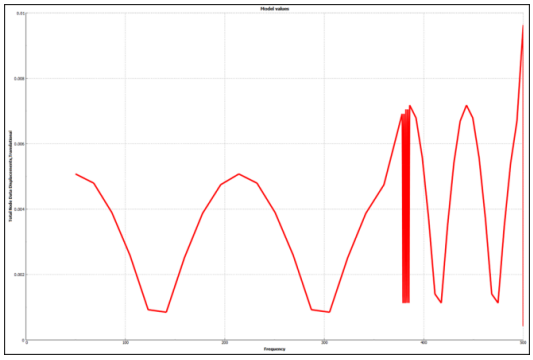

Figure 19: Displacements in Y direction

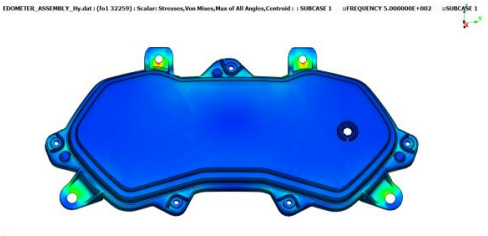

Figure 20: Stresses on Lens in Y direction

Similarly, the response of the system is maximum in Z direction at a frequency of 385.86 Hz. The value of maximum displacements observed at this frequency are 0.13mm which is below the permissible limit of 5mm moreover the resulting stresses at this frequency on the lens amount to 2.16 MPa which is below the fatigue limit by 88.75 %. The above is shown in figures 21 and 22 respectively.

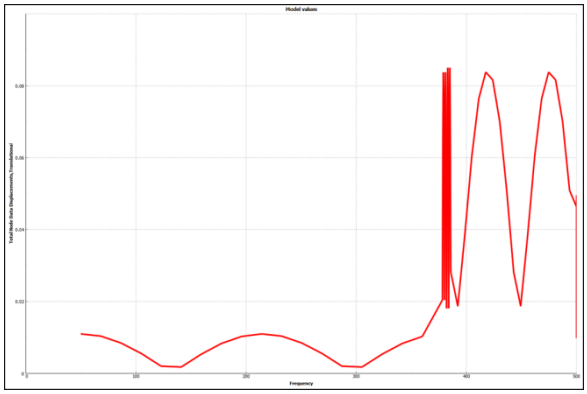

Figure 21: Displacements in Z direction

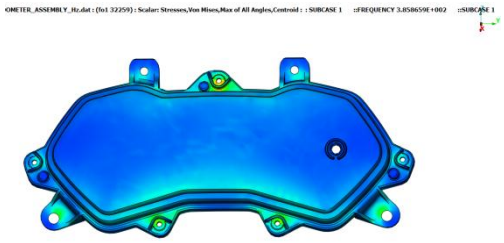

Figure 22: Stresses on Lens in Z direction

RESULTS AND DISCUSSIONS

A thorough understanding of the general material requirements for the Lens was established and different amorphous polymers were studied for their thermo mechanical properties, safety ratings, optical properties and environmental degradation retarding properties etc. An AMECA listen grade of PMMA was chosen as our material of choice. With the chosen material Mold Flow analysis was carried out to establish molding parameters and to check for any mold defects that could hamper the aesthetic region, following results were obtained from the mold flow.

- The single cavity old is filled with PMMA in 2.62 seconds with no short shot.
- The maximum pressure during injection is found to be 101.2 MPa which is within machine limit.
- Temperature at flow front rises by 10.6°C with no drop observed below the melt temperature of 235°C.
- Required clamping force is 138 tonnes.
- Shear rates are within material limit and prominent at the gate area.
- Air traps are found at the end fill locations and at the weld line locations.
- Weld lines are unavoidable and visible but strong as temperature at front doesn't fall below melt temperature.
- Volumetric shrinkage is found varying due to variable part thickness.
- Deflection observed (In X direction is +0.60mm & -0.59mm); (In Y direction is +0.35mm and -0.38mm); (In Z' direction is +0.23mm and -0.14mm).

Based on risk assessment derived from DFMEA static structural analysis was carried out for tightening torque at 2 locations namely vehicle-speedometer assembly mounting locations and lens-housing subassembly self-tapping screw locations. A factor of safety of 2 was chosen for the same. The results of both are represented in a tabular format below.

Results Summary					
Component	**Material**	**Loading Location**	**Torque(Nm)**	**Stress(MPa)**	**Result**
Speedometer	PMMA	Mounting Lug	1.3 Nm	11.4 MPa, 70.3 % below permissible	Safe
		Lens-Housing Screwing	0.45 Nm	5.37 MPa, 86% below permissible	Safe

Figure 23: Result Summary for tightening torque

A free-free modal analysis was carried out with meshed lens and housing with an equivalent mass placed at Cg location, the first 10 modal frequencies were called for the results. By the customer provided test standard only frequencies within 50-500 Hz range were of interest. The first modal frequency of 382.05 Hz fell within this range. Further harmonic response was carried out with a 10g acceleration value in X,Y,Z directions within the frequency range of interest including the first modal frequency. The results of the harmonic response are shown in tabular format in the figure below.

Material	Frequency	Maximum Stress Values @ Lens			Observed Stress as % of permissible	Result
		X direction	Y direction	Z direction		
PMMA	382.04 Hz	5.65 MPa	-	-	70.57 % below	Safe
	500 Hz	-	0.61 MPa	-	97 % below	
	385.86Hz	-	-	2.16 MPa	88.7 % below	

Figure 24: Stress Value Harmonic Response

Material	Frequency	Maximum Displacement Values						Result
		X direction	Limit X	Y direction	Limit Y	Z direction	Limit Z	
PMMA	382.04 Hz	0.32 mm	0.5 mm	-	0.5 mm	-	5 mm	Safe
	500 Hz	-		0.02 mm		-		
	385.86Hz	-		-		0.13 mm		

Figure 25: Displacement Values Harmonic Response

REFERENCES

[1] F.V.Loock et. Al Deformation and failure maps of PMMA in uniaxial tension, Engineering Department,Cambridge Univeristy,April 2018M. Young, The Technical Writer's Handbook. Mill Valley, CA: University Science, 1989.

[2] D.G. Gilbert, M.F. Ashby, P.W.R. Beaumont, Modulus-maps for amorphous polymers, J. Mater. Sci. 21 (1986) 3194–3210.K. Elissa, "Title of paper if known," unpublished.

[3] W.M. Cheng, G.A. Miller, J.A. Manson, R.W. Hertzberg, L.H. Sperling, Mechanical behaviour of poly(methyl methacrylate), J. Mater. Sci. 25 (1990).

[4] J.E. Mark, Physical Properties of Polymers Handbook, 3rd Ed., Cambridge University Press, 2003.

[5] G. Buisson, K. Ravi-Chandar, On the constitutive behaviour of polycarbonate under large deformation, Polymer (Guildf). 31 (1990) 2071–2076.

[6] L.S.A smith et. Al The effect of water on glass transition temperature of poly methyl methacrylate, Aachen 11th April 1998.

[7] Reimschuessel, H.K., 1977. Nylon 6.Chemistry and mechanisms. Journal of Polymer Science: Macromolecular Reviews, 12(1), 65-139.

[8] K. P. Menard, Dynamic Mechanical Analysis: A practical introduction, Bocaraton: CRC press LLC, 1999.

[9] V. Shaktawat, N. Jain, N.S. Saxena, K. B. Sharma and T.P. Sharma, J. Poly. Sci. Series B 49, 236-239 (2007).

[10] M. Dixit, V. Shaktawat, K. B. Sharma, N.S. Saxena and T.P. Sharma, "Mechanical Characterization of Poly methyl methacrylate and Polycarbonate Blends" in Thermophysical Properties of Materials and Devices-NCTP '07, edited by P. Predeep et al., AIP Conference Proceeding 1004, American Institute of Physics, Melville, NY, 2008, pp. 311-315

[11] S. Agarwal et. Al Investigation of thermo-mechanical properties of PMMA,.,Semi conductor and Polymer Science Laboratory,University of Rajasthan, 2010.

[12] J.Rosler,H.Harders,M.Ba€ker,Mechanical behaviour of polymers, Mechanical Behaviour of Engineering Materials Metals, Ceramics, Polymers, and Composites, Springer, Berlin, 2007.

[13] E.M. Arruda, M.C. Boyce, R. Jayachandran, Effects of strain rate, temperature and thermomechanical coupling on the finite strain deformation of glassy polymers, Mech. Mat. 19 (1995) 193e212.

[14] A.D. Mulliken, M.C. Boyce, Mechanics of the rate-dependent elasticeplastic deformation of glassy polymers from low to high strain rates, Int. J. Solids Struct. 43 (2006) 1331e1356. 99 [15] ISO 527-1, Plastics Determination of Tensile Properties - Part 1: General Principles, ISO, 2012.

[15] S. Ataya et.al Temperature Dependent Mechanical Behavior of PMMA: Experimental Analysis and Modelling,April 2017

[16] Henzi P, Rabus DG, Bade K, Wallrabe U, Mohr J. Proc. SPIE 2004; 5454: 64-7